JOURNAL OF GEOPHYSICAL RESEARCH, VOL. 113, D06113, doi:10.1029/2007JD008548, 2008

The SAFRAN-ISBA-MODCOU hydrometeorological model applied over France

F. Habets,[1,2] A. Boone,[1] J. L. Champeaux,[1] P. Etchevers,[3] L. Franchistéguy,[1] E. Leblois,[4] E. Ledoux,[5] P. Le Moigne,[1] E. Martin,[1] S. Morel,[6] J. Noilhan,[1] P. Quintana Seguí,[1] F. Rousset-Regimbeau,[1] and P. Viennot[5]

Received 15 February 2007; revised 20 June 2007; accepted 16 November 2007; published 29 March 2008.

[1] The hydrometeorological model SIM consists of a meteorological analysis system (SAFRAN), a land surface model (ISBA), and a hydrogeological model (MODCOU). It generates atmospheric forcing at an hourly time step, and it computes water and surface energy budgets, the river flow at more than 900 river-gauging stations, and the level of several aquifers. SIM was extended over all of France in order to have a homogeneous nationwide monitoring of the water resources: it can therefore be used to forecast flood risk and to monitor drought risk over the entire nation. The hydrometeorological model was applied over a 10-year period from 1995 to 2005. In this paper the databases used by the SIM model are presented; then the 10-year simulation is assessed by using the observations of daily streamflow, piezometric head, and snow depth. This assessment shows that SIM is able to reproduce the spatial and temporal variabilities of the water fluxes. The efficiency is above 0.55 (reasonable results) for 66% of the simulated river gauges, and above 0.65 (rather good results) for 36% of them. However, the SIM system produces worse results during the driest years, which is more likely due to the fact that only few aquifers are simulated explicitly. The annual evolution of the snow depth is well reproduced, with a square correlation coefficient around 0.9 over the large altitude range in the domain. The streamflow observations were used to estimate the overall error of the simulated latent heat flux, which was estimated to be less than 4%.

Citation: Habets, F., et al. (2008), The SAFRAN-ISBA-MODCOU hydrometeorological model applied over France, *J. Geophys. Res.*, *113*, D06113, doi:10.1029/2007JD008548.

1. Introduction

[2] Interfacing a Soil Vegetation Atmosphere Transfer Scheme (SVAT) with streamflow routing model permits the assessment of the water and energy budgets simulated by SVAT schemes, and the identification of their main qualities and defects. This has been done extensively in order to assess global and regional climate models [*Miller et al.*, 1994; *Benoit et al.*, 2000], as well as in SVAT intercomparison experiments. For instance, the Pilps2c experiment [*Wood et al.*, 1998; *Lohmann et al.*, 1998] showed the importance of the parameterization of subgrid runoff for simulating a realistic hydrograph. The Rhone-Agg intercomparison study [*Boone et al.*, 2004] showed that in the Alps, the SVATs that use explicit snow schemes (with an explicit simulation of the energy budget of the snowpack) obtain better results than those using composite snow schemes (i.e., one single energy budget for both the snow-free and snow covered part of the ground surface). Results of the DMIP1 (distributed model intercomparison model [*Reed et al.*, 2004]) show that among the participant distributed hydrological models, the few that simulated both the water and the energy budgets (NOAH [*Chen et al.*, 1997]; VIC-3L [*Liang et al.*, 1994]; and tRIBS [*Ivanov et al.*, 2004]) obtained similar results in terms of the simulation of the river flows as the others. Thus, although SVAT schemes were originally dedicated to providing surface energy fluxes to an atmosphere model, they are now also able to make an accurate estimation of the hydrological cycle at both short and long timescales.

[3] Several studies focusing on the soil moisture assimilation for numerical weather prediction models have used SVAT off-line simulations (i.e., uncoupled to the atmosphere) forced by observed data, in combination with satellite and/or surface atmospheric data assimilation to estimate mesoscale soil moisture over large areas (European Land Data Assimilation System (ELDAS), B. J. J. M. Van der Hurk et al., ELDAS Final Report December 2001 to December 2004, 2005, available at http://www.knmi.nl/samenw/eldas/; North American Land Data Assimilation

[1]GAME/CNRM, Météo-France, CNRS, Toulouse, France.
[2]Now at UMR-Sisyphe 7619, Université Paris VI, CNRS, Paris, France.
[3]GAME/CEN, Météo-France, CNRS, Saint Martin d'Heres, France.
[4]CEMAGREF, Lyon, France.
[5]Centre de Geosciences, ENSMP, ParisTech, Fontainebleau, France.
[6]DIRIC, Météo-France, Paris, France.

0148-0227/08/2007JD008548$09.00

System (NLDAS) [*Mitchell et al.*, 2004]). One key aspect of such studies is the retrieval of the best surface near realtime atmospheric forcing. However, both studies include a retrospective period in order to test the ability of the method to compute consistent surface fluxes and river flow over long time periods. In NLDAS, the SVAT schemes are also coupled to a hydrological routing model in order to assess the SVAT scheme simulations of the water budget over large areas, through comparison with observed river flows.

[4] The CNRM-GAME has been developing SVAT scheme and soil moisture assimilation techniques for over the last 10 years, in order to provide surface boundary conditions to the atmosphere models. For instance, CNRM-GAME takes part in the ELDAS and Canadian Land Data Assimilation System (CALDAS) [*Balsamo et al.*, 2006] projects using the ISBA surface scheme. It has also, in association with the Mining school of Paris, developed the SIM hydrometeorological model that is used both for realtime estimation of the soil moisture, and for retrospective studies of the water and energy budgets for a region covering all of France.

[5] The SIM (SAFRAN-ISBA-MODCOU) model is the combination of three independent parts: (1) SAFRAN [*Durand et al.*, 1993]), which provides an analysis of the atmospheric forcing, (2) ISBA [*Noilhan and Planton*, 1989; *Boone et al.*, 1999], which computes the surface water and energy budgets, and (3) MODCOU [*Ledoux et al.*, 1989], which computes the evolution of the aquifers and the river flow.

[6] The SIM system was first tested for large French catchments: the Adour [*Habets et al.*, 1999c], the Rhone [*Etchevers et al.*, 2001b], the Garonne [*Voirin-Morel*, 2003, available at http://www.cig.ensmp.fr/hydro/THE/the.htm] and the Seine basins [*Rousset et al.*, 2004], and the Maritsa river basin in Bulgaria [*Artinyan et al.*, 2008]. It has been used to quantify the influence of the snowpack, groundwater, soil moisture, and urbanized areas on certain flood events of the Seine basin [*Rousset et al.*, 2004]. SIM has also been used to study the evolution of the water resources in a climate change prospective [*Etchevers et al.*, 2002; *Caballero et al.*, 2007].

[7] SIM was extended over all of France in 2002, and it has been used operationally at Météo-France since 2003 in order to monitor the water resources at the national scale in near real time. In order to assess the quality of the SIM system over France, a retrospective run was made for the period 1995 to 2005, and the goal of this article is to present the results of the SIM hydrometeorological model over this period. First, the SIM system is presented, with a summary of the main innovations compared to the previous studies. Then, the database is presented, with a special emphasis on the atmospheric data, which is critical in terms of the quality of the entire system. The assessment is based on observed river flow, piezometric head, and snow depth. Finally, the spatial and temporal evolutions of the water and energy fluxes on the main basins are presented.

2. The SIM Hydrometeorological Model

[8] The SIM (SAFRAN-ISBA-MODCOU) system consists in three independent modules (Figure 1).

2.1. SAFRAN Analysis System

[9] The SAFRAN analysis system [*Durand et al.*, 1993] was developed in order to provide an analysis of the atmospheric forcing in mountainous areas for the avalanche forecasting. SAFRAN analyses eight parameters: the 10-m wind speed, 2-m relative humidity, 2-m air temperature, cloudiness, incoming solar and atmospheric radiations, snowfall and rainfall. A detailed description and assessment of the SAFRAN analysis over France is presented by *Quintana Seguí et al.* [2008], so that only the main aspects are summarized herein.

[10] The main hypothesis of SAFRAN is that the atmospheric variables are considered to be homogeneous over some well-defined areas, within which they can only vary according to the topography. In France, these areas correspond to the Symposium homogeneous climate zones which are used at Météo-France for weather forecast bulletins. There are about 600 homogeneous climate zones, each with an average area around of 1000 km^2, so that each zone contains at least two rain gauges and one surface meteorologic station.

[11] SAFRAN takes into account all of the observed data in and around the area under study. For instance, there are more than 1000 meteorological stations for the 2-m temperature and humidity, and more than 3500 daily rain gauges, which corresponds to about six rain gauges for each climate zone. For each variable analyzed, an optimal interpolation method is used to assign values to given altitudes within the zone. According to the altitude of the observations, SAFRAN provides a single vertical profile of the variable within the zone with a vertical resolution of 300 m.

[12] The analysis are computed every 6 h, and the data are interpolated to a hourly time step.

[13] The incoming radiative fluxes and the precipitation (liquid and solid) are treated differently.

[14] The precipitation rate is estimated daily using 3500 daily rain gauges, and then interpolated hourly, based on the evolution of the air relative humidity (precipitation is constrained to occur when the relative humidity is high). The partition between snowfall and rainfall is based on the 0.5°C isotherm: the precipitation is considered as snowfall if the air temperature is below 0.5°C.

[15] The radiation scheme of *Ritter and Geleyn* [1992] is used to compute the incoming radiation fluxes since there are few in situ observations available. The method requires an estimate of the cloudiness which is analyzed using, as a first guess, the operational analysis of Numerical Weather Prediction model, and in situ observations.

[16] Once the vertical profile of the atmospheric parameters have been computed in each homogeneous zone, the values are interpolated in space as a function of the altitude of each grid cell within each homogeneous zone.

2.2. ISBA Land Surface Scheme

[17] The ISBA land surface scheme [*Noilhan and Planton*, 1989; *Noilhan and Mahfouf*, 1996] is used in the NWP, research and climate models at Météo-France. In order to fulfill all its applications, the ISBA surface scheme is quite modular. In the SIM system, the three-layer force

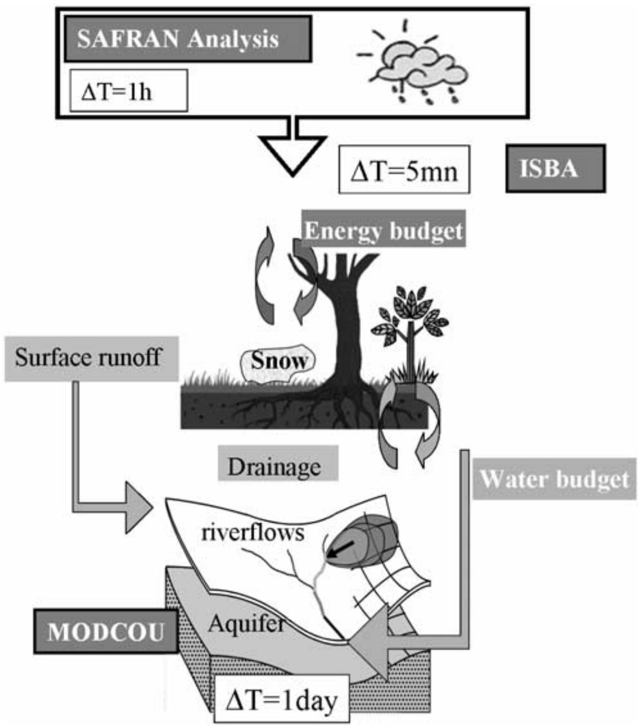

Figure 1. The SIM hydrometeorological model consists in of three independent modules: the SAFRAN atmospherical analysis, the ISBA land surface model, and the MODCOU hydrogeological model.

restore model is used [*Boone et al.*, 1999], together with the explicit multilayer snow model [*Boone and Etchevers*, 2001]. Moreover, the subgrid runoff [*Habets et al.*, 1999b] and subgrid drainage schemes [*Habets et al.*, 1999a] are used. This last parameterization is quite simple, and allow to indirectly take into account the impact of unresolved aquifers on the low river flows based on a single parameter.

[18] The soil and vegetation parameters used by ISBA are derived from the ECOCLIMAP database [*Masson et al.*, 2003] (see section 3.2). Only two parameters in ISBA are not directly defined by the soil and vegetation classification: the subgrid runoff parameter and the subgrid drainage parameter, w_{drain}.

[19] The subgrid runoff parameter was assigned the default value in the current study as was the case for the other SIM applications. Only the subgrid drainage parameter was calibrated in this application. In previous simulations, this subgrid parameter was either set to a default value [*Habets et al.*, 1999a], or calibrated to optimize the Nash criteria [*Etchevers et al.*, 2001b], or the discharge for the summer low-flow period [*Caballero et al.*, 2007]. In the France application, it is calibrated using the method presented by *Caballero et al.* [2007] in order to sustain the observed Q10 quantile of the river flow. The subgrid drainage parameter is simply set using the expression

$$Q10 = \sum_i C_{3_i}/\tau \times w_{drain} \times d_i \times S_i$$

where i represents the grid cells that belong to the upstream area of the river gauge under study, C_{3_i} is the gravitational drainage coefficient for the grid cell i, d_i the soil depth for the grid cell i, S_i is the surface of the grid cell i that belong to the upstream area of the river gauge under study, and τ a time constant of 1 d. In this expression, C_{3_i} and d_i only depend on the soil and vegetation database, and $Q10$ is set at each simulated river gauge using the statistics provided over the entire observation period for each station. Thus, the value of the subgrid drainage coefficient is defined using observed data and the physiographic database, and is thus unique once these databases are defined. Therefore, there is no iteration for the calibration, and thus, no "calibration period."

[20] The surface scheme is linked to the MODCOU hydrogeological model by the ISBA output soil water fluxes: The drainage simulated by ISBA is transferred to MODCOU as the input flow for the simulation of the evolution of the aquifer, while the surface runoff computed by ISBA is routed within the hydrographical network by MODCOU to compute the river flow.

2.3. MODCOU Hydrogeological Model

[21] The MODCOU hydrogeological model computes the spatial and temporal evolution of the piezometric level of multilayer aquifers, using the diffusivity equation [*Ledoux et al.*, 1989]. It then computes the exchanges between the aquifers and rivers, and finally it routes the surface water within the river, using a simple isochronism algorithm (Muskingum), to compute river flows. In the SIM-France system, the river flow is computed at a 3-h time step (instead of daily as in the previous applications), and the evolution of the aquifer is computed daily.

[22] ISBA snowpack, soil temperature, and soil moisture values are initialized using a 1-year spin-up (the first year is repeated twice), whereas the initial conditions of the aquifers are taken from the Rhone and Seine basin applications.

[23] In section 3, a short description of the database is presented.

3. Databases Used

[24] The databases for the SIM-France application use the Lambert II projection, which has the advantage of preserving the surface area. SIM uses input data that have different spatial resolutions: a regular 8 km grid is used by SAFRAN and ISBA, and irregular embedded grid cells varying in size from 1 to 8 km are used by MODCOU (the highest resolution is associated with rivers and basin boundaries).

3.1. Hydrogeologic Database

[25] The hydrographic network was derived from the USGS GTOPO30 elevation database at a 1-km resolution. The slope is used to derive the direction of the flow, and to compute the drainage area of each cell.

[26] The topography at the 8-km resolution, the river network, and the main basins are shown in Figure 2. The river network extends over approximately 42,000 km, which represents about 12% of the 194,000 mesh points of the hydrographic network.

[27] More than 900 river gauges are taken into account in the river flow simulations, with an upstream area ranging from 240 km^2 to 112,000 km^2.

[28] Currently, the aquifers of only two basins have been simulated: the three aquifer layers of the Seine basin, and

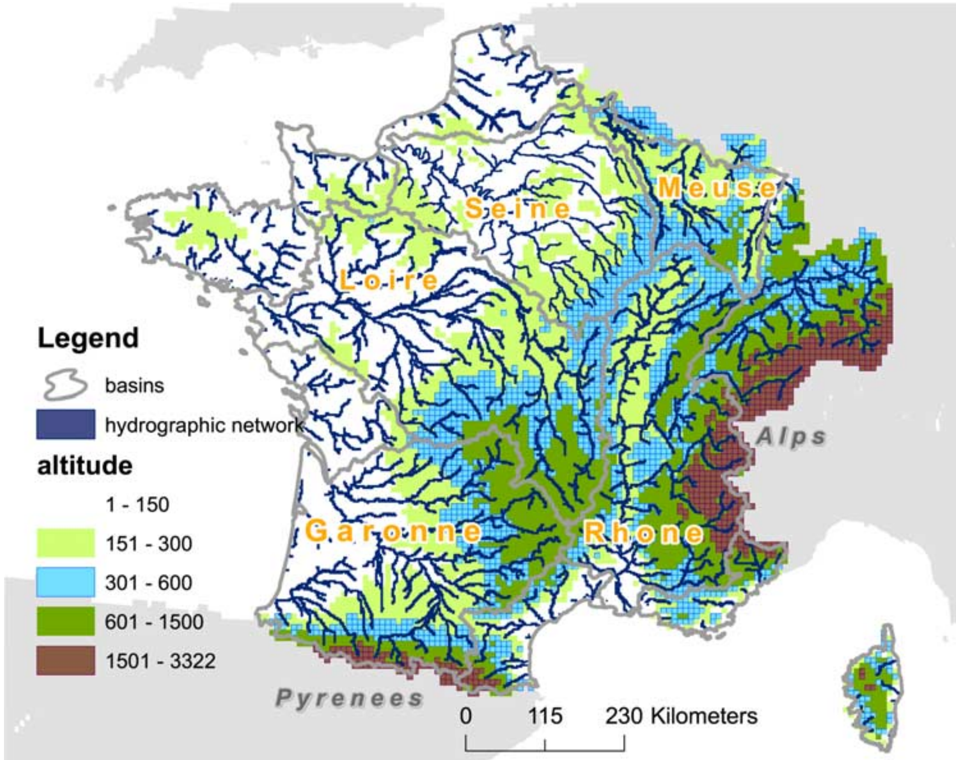

Figure 2. Topography and hydrographic network.

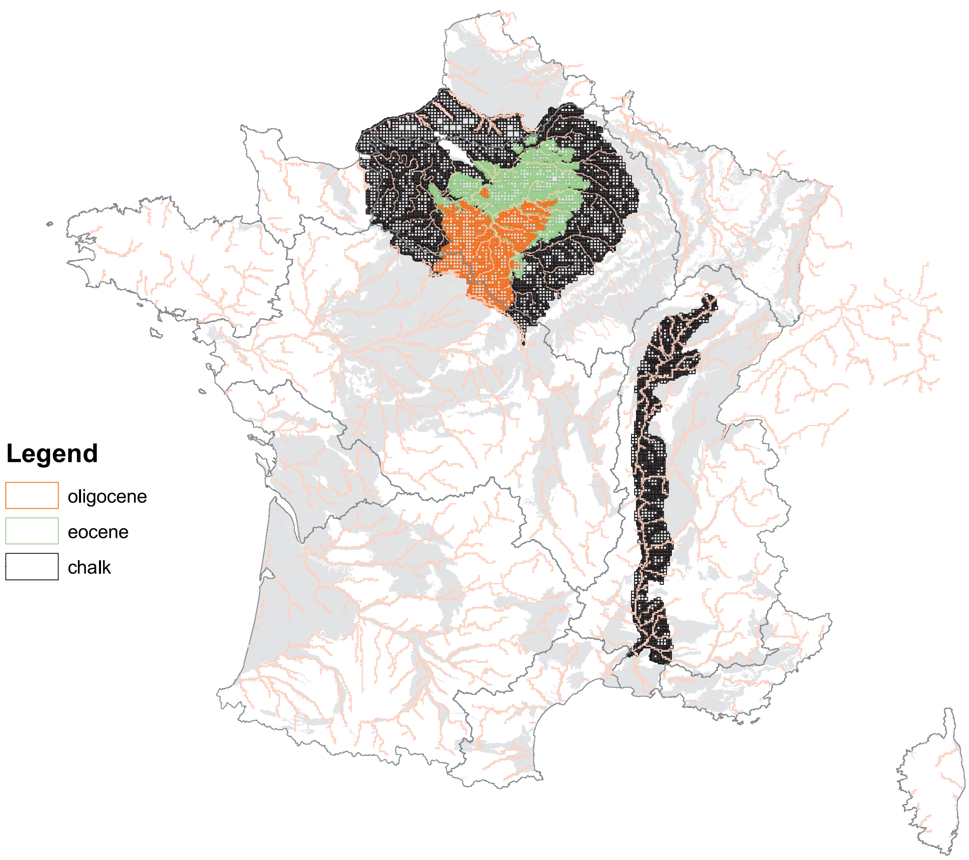

Figure 3. Simulated aquifers (cells) and main aquifers as defined in the Base de Données sur le Référentiel Hydrogéologique Français (BDRHF; http://sandre.eaufrance.fr) hydrogeological database (dashed).

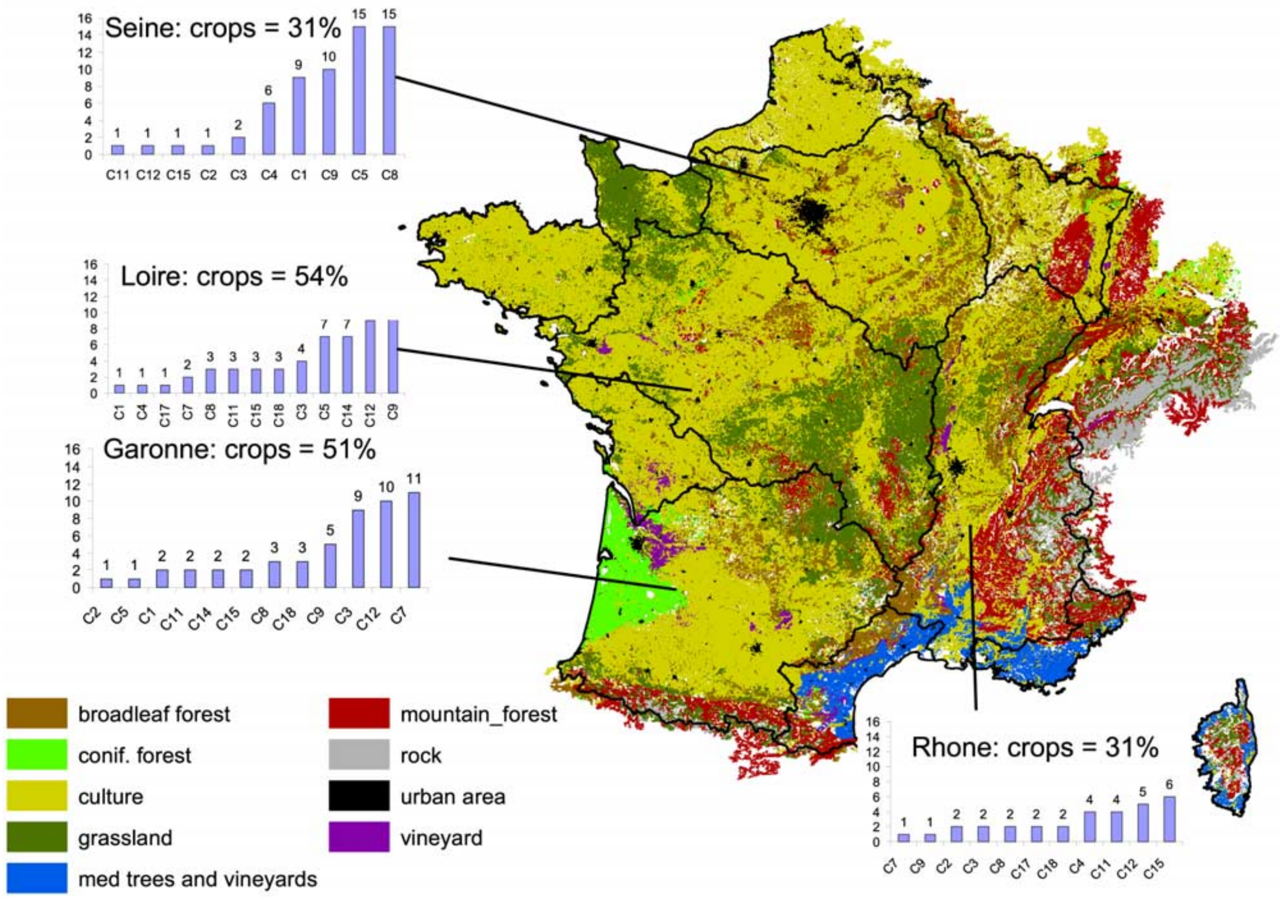

Figure 4. The main types of vegetation from the ECOCLIMAP-France database.

the single aquifer layer of the Rhone basin (Figure 3). The aquifer parameters were calibrated by *Gomez et al.* [2003] and *Golaz-Cavazzi et al.* [2001], respectively, and were already used in previous applications of SIM for these basins.

[29] However, aquifers are more widespread in France. The main aquifers defined in the French Hydrogeological Reference database (BD RHF, http://sandre.eaufrance.fr) and those simulated are shown in Figure 3. In those areas where an aquifer is present but not explicitly simulated

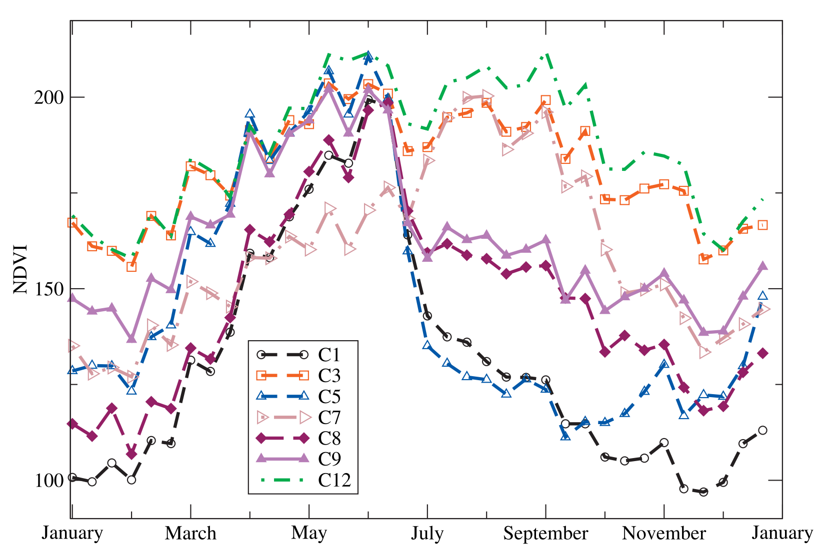

Figure 5. The 10-d evolution of the NDVI for the main crop types.

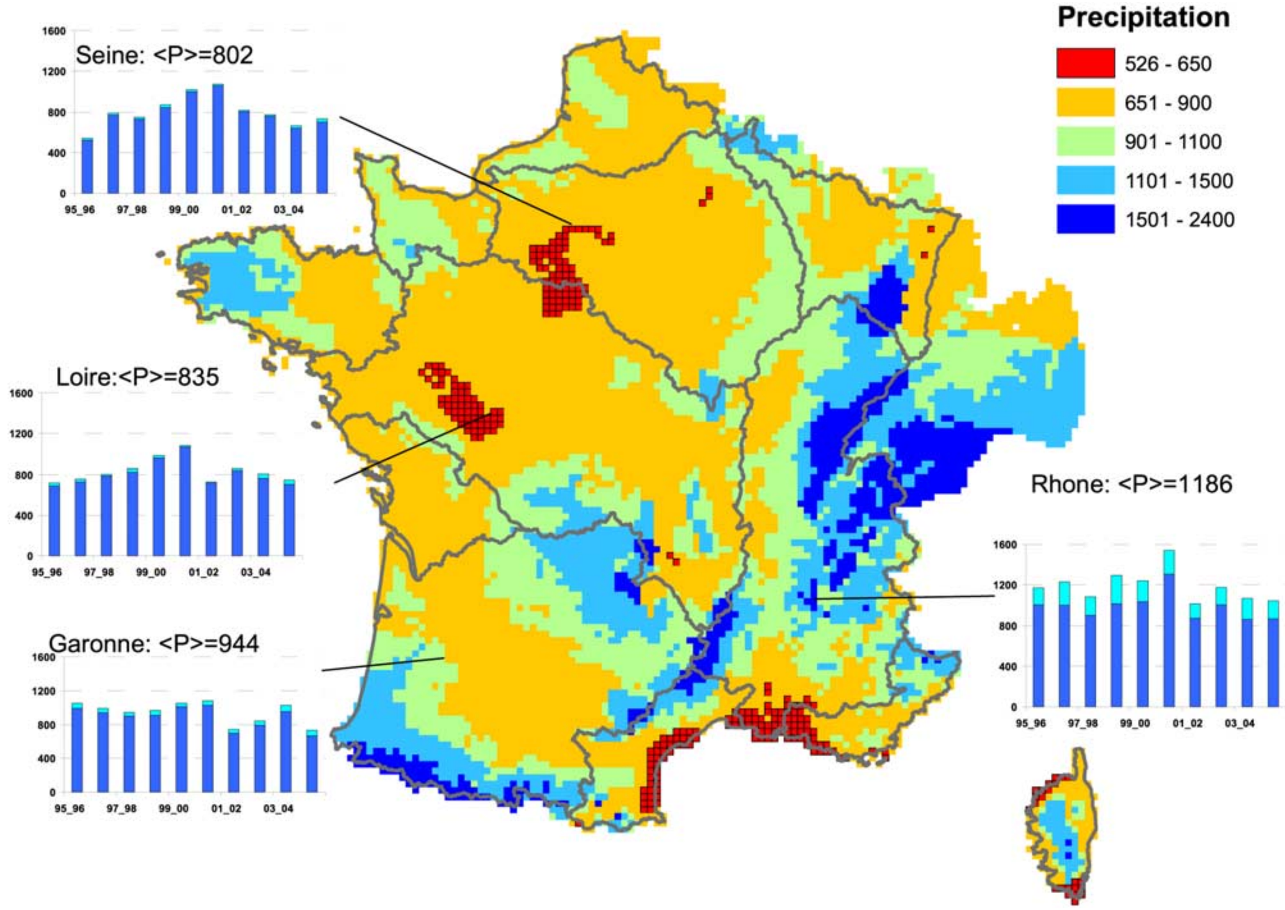

Figure 6. Mean annual precipitation in mm/a. The encapsulated graph presents the annual precipitation for each year on average over the selected basin.

(grey shaded areas in Figure 3), the subgrid drainage parameter was calibrated in order to sustain the summer river flows. Everywhere else, the parameter is set to 0.

3.2. Soil and Vegetation Parameters for ISBA

[30] The ISBA parameters are derived from the ECOCLIMAP database [*Masson et al.*, 2003]. However, an improved version of the ECOCLIMAP database was developed for the SIM application.

[31] This database uses a Lambert II projection at a 1-km resolution for both the vegetation and the soil parameters (as opposed to approximately 10 km for the soil map in the global ECOCLIMAP database).

[32] The vegetation classification (Figure 4) is based on the Corine Land Cover (CLC) 1990 database, associated with a climate map [*Masson et al.*, 2003]. This database is quite accurate for the forested areas, vineyards and urban areas, but it does not distinguish the various crops that are aggregated into a single class and distributed over very large domains. In order to be able to distinguish winter and summer crops, as was done in the Adour study [*Habets et al.*, 1999b], it was decided to better define the crop classes, using the 10-d Normalized Vegetation Index (NDVI) archive of SPOT/VEGETATION for the year 2000 at a 1km resolution. Using differences in the NDVI profiles, the crop classes of Corine were split into 20 subsets (referred as C1, C2, to C20 in the following). The distribution of these crop types within the main basins is presented Figure 4. Among the large basins, the Seine basin is the most cultivated, with 60% of the surface covered by crops. The Loire and Adour-Garonne basins have about the same crop surfaces (54 and 51%, respectively), whereas the Rhone basin is the least cultivated large basin (31%), primarily because the eastern part of the basin is mountainous.

[33] The crop partition is different within each basin: the two dominant crop types represent half of the cultivated area of the Seine basin, while in the other basins, it represents only one fifth (Figure 4).

[34] The 10-d NDVI cycles of the dominant crop types are presented in Figure 5. The NDVI cycle cannot be used to directly identify the type of the crop class, however the class C7, which is dominant in the Adour-Garonne basin with a maximum NDVI from July to September, is representative of summer crops, especially Maize. In contrast, the C1 class, with a very narrow cycle, and which is mostly present in the north of France, is associated with winter crops, such as wheat, as well as the classes C8 and C9 dominant in the Seine and Loire basins.

[35] In order to derive the ISBA vegetation parameters, the ECOCLIMAP correspondence tables were used. The annual leaf area index (LAI) cycle is based on the 10-d NDVI tendencies, with the extreme values of the LAI fixed for each vegetation type (from 0 to 4 m^2/m^2 for crops). Then the 10-d evolution of the vegetation fraction, roughness

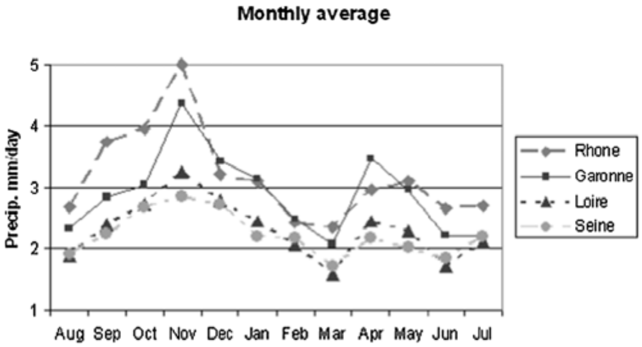

Figure 7. Mean monthly precipitation averaged on the main basin.

length, and albedo are derived using the formulations given by *Masson et al.* [2003]. For the other vegetation types, the annual cycle was recomputed at a 10-d time step instead of the monthly time step used in the ECOCLIMAP global database.

[36] The soil map used in the ECOCLIMAP France database is taken from the Institut National de Recherche Agronomique (INRA) 1-km soil geographical database (Base de données géographique des Sols de France (BDGSF) http://www.gissol.fr/programme/bdgsf/bdgsf.php). Only the percentages of sand and clay are used to define the soil parameters for ISBA [*Noilhan and Lacarrère*, 1995].

3.3. Atmospheric Database

[37] Data from more than 1000 surface meteorological stations and more than 3500 daily rain gauges were analyzed by the SAFRAN system. SAFRAN has been used to produce an atmospheric database at an hourly time step over the France domain, for the period starting in August 1995 and ending in July 2005. A detailed presentation and assessment of the eight variables analyzed by SAFRAN for the years 2001–2002 and 2004–2005 is given by *Quintana Seguí et al.* [2008]. Therefore, only the main characteristics of the 10-year precipitation database are presented here.

[38] The mean annual precipitation over the 10-year period is shown Figure 6. As can be expected, precipitation is abundant in the mountains, and also, along the Atlantic coast. The southeastern border of the Massif Central experiences heavy rainfall primarily in the fall season which leads to significant annual precipitation totals.

[39] The Seine and Loire basins in the north receive less precipitation (802 and 835 mm/a, respectively) than the southern basins that are more mountainous (944 and 1186 mm/a for the Garonne and Rhone basins, respectively). The year 2000–2001 is the wettest for all of the basins, and the year 2001–2002 is the driest for all basins except the Seine (encapsulated graphs in Figure 6). Snowfall is shown in Figure 6 as light blue at top of each histogram. It is a key component of the Rhone basin precipitation and comprises 29% of the total. Despite the presence of the Pyrenees mountain range, snowfall is less significant in the Adour-Garonne basin, where it represents only 5.7% of the total precipitation. It represents less than 3% in the two other basins.

[40] The monthly cycle of precipitation presents a similar pattern for almost all the basins on average over the 10 years. Precipitation has two maxima in the year: one in winter, and one in spring (Figure 7). The cycle is less pronounced for the northern basins, where the average rainfall ranges from 1.58 to 3.2 mm/d in March and November, respectively, than in the southern basins where it ranges from 2 to 5 mm/d.

4. Evaluation of the Hydrometeorological Modeling

[41] The 10-year integration of the SIM system was assessed using various data, either local or spatially integrated, and either instantaneous or averaged over a certain time period. This section presents the comparison of the simulation with the daily observed river flows, the piezometric levels and the snow depths.

4.1. Comparison With Observed River Flow

[42] Figure 8 presents the daily river flows at the river gauges located closest to the outlet of the four largest rivers of France which are not affected by the tide (the location of the river gauges can be seen Figure 10). The observed river flows are plotted using dark circles, and the simulation is represented by the continuous lines. The Garonne at Lamagistere has the smallest upstream area (50,430 km^2), and logically has the lowest average discharge, but it has higher flood peaks than the Seine basin at Poses (which has an upstream area of 65,686 km^2). This is due to the fact that the Garonne encompasses part of the Pyrenees and Massif Central mountains, where heavy orographically enhanced precipitation can occur, while the Seine basin overlays a widespread aquifer, which tends to reduce the winter flood peaks and to sustain the summer low flow. The Loire at Montjean sur Loire, which has the largest upstream area (110,356 km^2) has an average discharge almost two times lower than that of the Rhone at Beaucaire, which has a smaller contributive area (96,412 km^2). This results because the Rhone basin encompasses part of several mountain ranges, notably the Alps. The Rhone rivers had two large flood events during the period under investigation in December 2002, and December 2003. Unfortunately, observed discharge data have not been available at Beaucaire since 2003.

[43] SIM is capable of representing the dynamic of the flows measured at these four river gauges. However, some deficiencies can be seen. For instance, SIM tends to underestimate the summer flow of the Rhone at Beaucaire. This is mainly due to the fact that the model does not take into account the numerous dams used for hydroelectricity power in the Alps which tend to sustain the summer flow. As for the Garonne and Loire rivers, the recession of the flood peaks are too fast in the model. This is partially due to the fact that the main water tables are not simulated in those two basins.

[44] To quantify the ability of the SIM system to represent the daily river flows, two statistical results are used: the discharge ratio (q_{sim}/q_{obs}) and the efficiency, E [*Nash and*

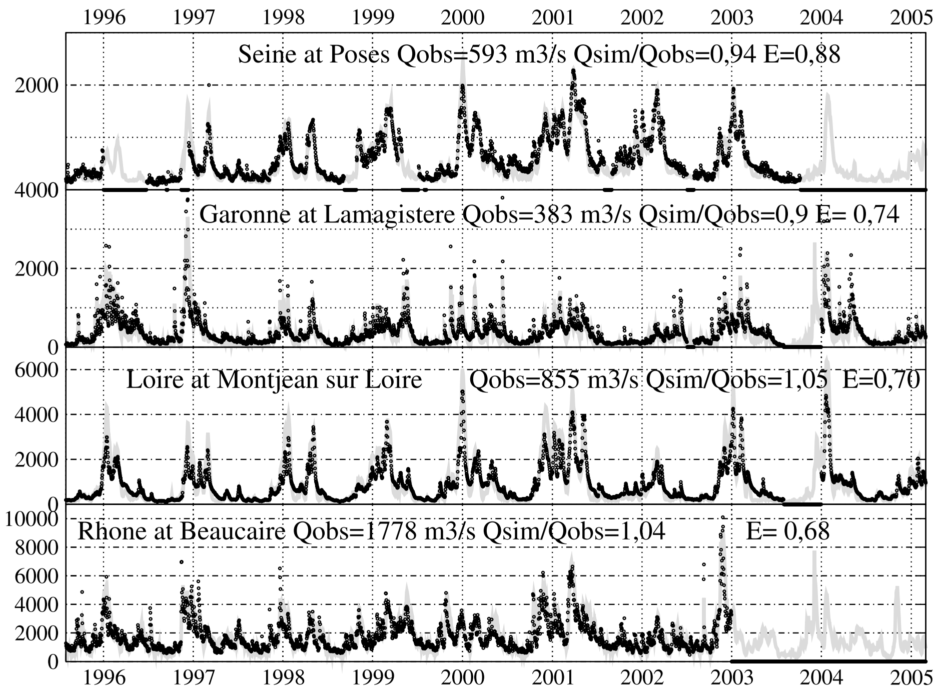

Figure 8. Daily observed (black circle) and simulated (line) river flows at the outlet of the four main rivers. The scale varies for each gage. The title includes the mean observed discharge on the period *Qobs*, the discharge ratio *Qsim*/*Qobs*, and the efficiency E.

Sutcliffe, 1970]. These statistical criteria were computed at a daily time scale over the full period with available observations. The SIM system is able to simulate the river flows at the outlet of these four main basins with a good accuracy, corresponding to an efficiency ranging from 0.68 to 0.88, and an error on the discharge ranging from −10% to +6%.

[45] Figure 9 presents the results obtained by SIM over 610 river gauges with available data, as a function of the

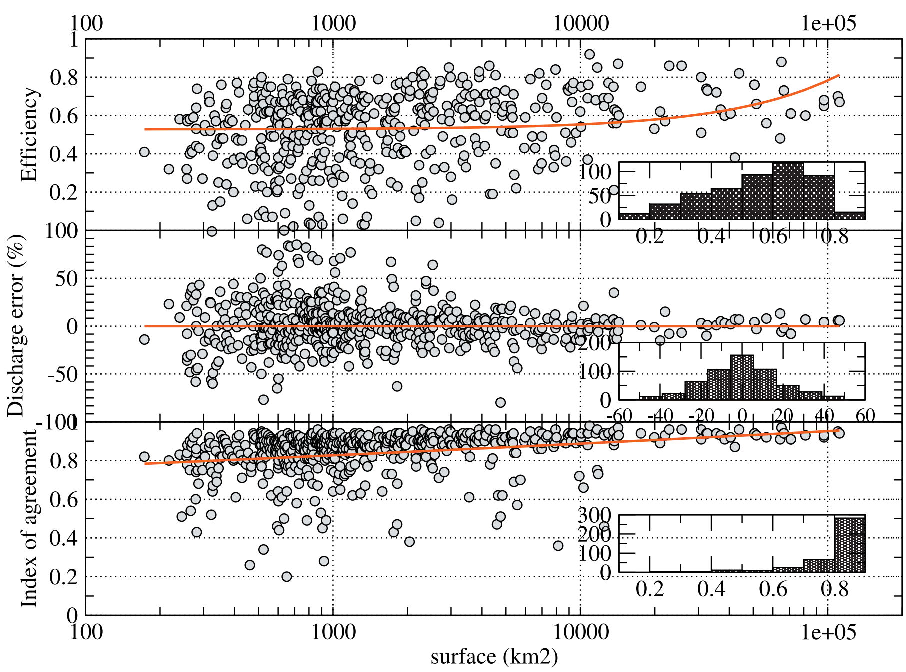

Figure 9. (top) Efficiency, (middle) discharge error, and (bottom) index of agreement for each simulated river gauges plotted versus the upstream area of the river gauges. The circles represent the river gauges, and the line is the linear regression (x axis is log). The encapsulated graphs represent the histogram of the statistical results.

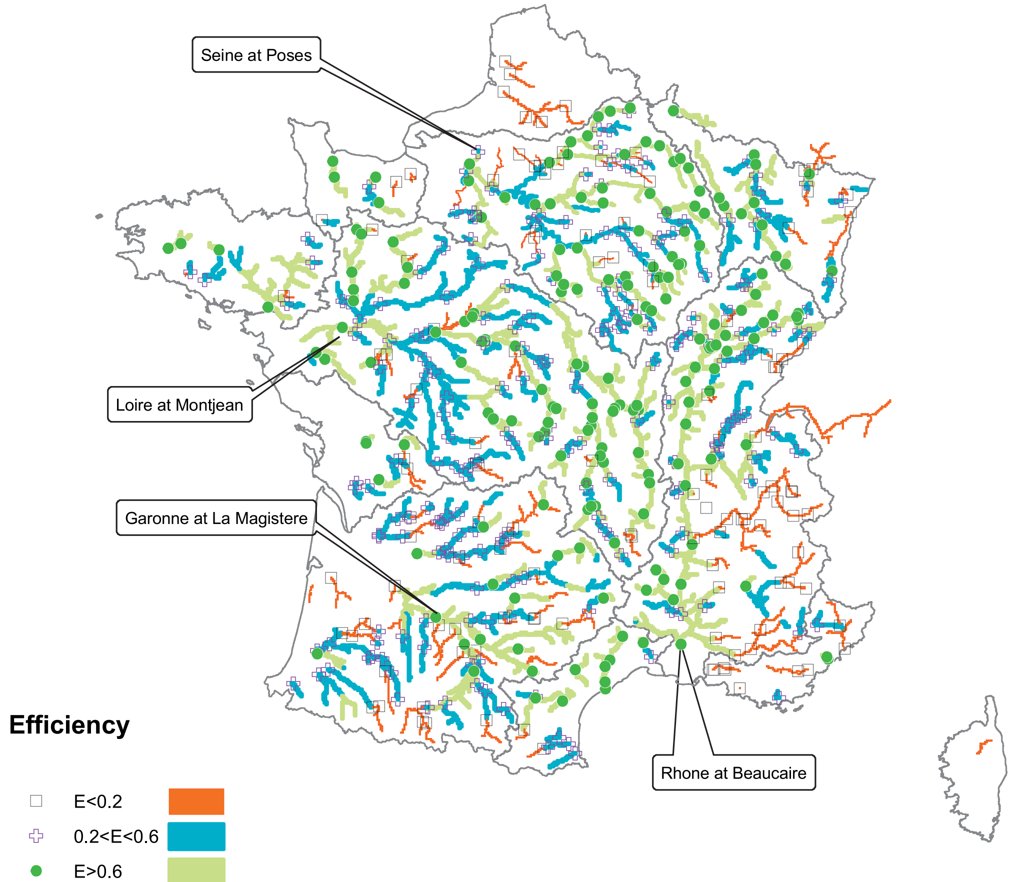

Figure 10. Spatial representation of the efficiency for each river gauge and the corresponding river network.

surface of the river gauge basin. Each circle represents a river gauge, and the linear regression line is shown (it appears as an exponential, due to the log x axis unit). Of course, there are more stations with a small area (below 1000 km^2), than with a large area (above 10,000 km^2). The index of agreement [*Willmot*, 1981] is above 0.8 for most of the river gauges, and there are few river gages with an index of agreement below 0.6. In general, the bad results for these stations are due to the fact that either the river is influence significantly by dams (e.g., Durance and Isere rivers), or that they are have nonnegligible interaction with a large aquifer that is not explicitly taken into account (e.g., Somme and Leyre rivers). There is a clear link between the quality of the simulation and the surface of the river basin: Figure 9 shows that the average efficiency is close to 0.5 for the small river stations, while it is around 0.7 for the larger ones. Moreover, there is a larger ratio of river gauges with a very good efficiency (above 0.8) for the larger basins. There are several factors that lead to the overall better results for the large basins. One key point is that the forcing data has larger errors for small basins (essentially the precipitation). In the large basins, some errors in the upstream basin can be compensated for downstream, leading to overall better results. The same kind of compensation can occur for the description of the geological and surface properties. An additional reason could be that the human activities (dams, derivation, pumping, etc.) can have relatively larger effect on the small basin discharge. Finally, larger errors may be due also to the faster hydrologic response of those basins which cannot be reproduced by the relatively simple river routing model used herein.

[46] The encapsulated graph presents the histogram of the efficiency. The maximum of the histogram is reached for an efficiency between 0.6 and 0.7 (121 river gauges). 101 river gauges have an efficiency above 0.7, and only 20 have values above 0.8. That implies that more than 36% of the river gauges was associated with a daily efficiency over the full period that can be considered as "rather good" ($E > 0.6$), and 16% as "fair" ($E > 0.7$).

[47] Another 30% of the river gauges have an efficiency that can be considered as reasonable ($0.55 < E < 0.65$). There are 97 stations with an efficiency below 0 (very poor, not shown in Figure 9), which represents 15% of the river gauges, and is comparable to the large-scale study by *Henriksen et al.* [2003]. This subset includes all of the river gauges which are significantly affected by dams.

[48] The discharge error is close to zero on average, but is more scattered for the small basins than for the larger basins. The encapsulated histogram is centered on zero, which is consistent with the results of the regression fit.

[49] Figures 10 and 11 present the spatial repartition of the efficiency and of the discharge ratio, with the results at each gage and their associated river network. As expected, the results are quite good for the main rivers. Nonetheless,

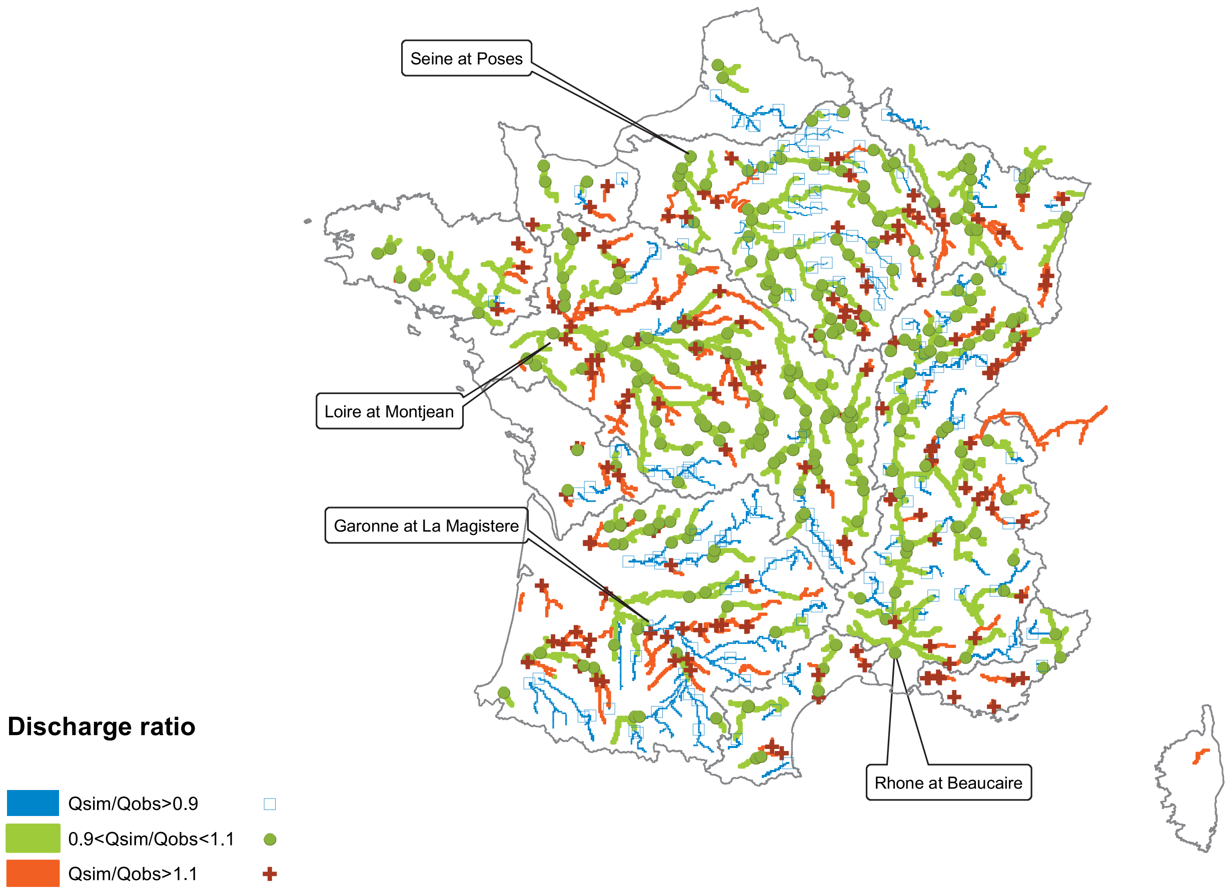

Figure 11. Spatial representation of the discharge ratio for each river gauges and the corresponding river network.

some areas have poor results in terms of efficiency: notably the Alps and the northern portion of the domain. For the Alps, this is mainly due to the fact that this region is used to produce hydropower, and the natural river flows are perturbed by numerous dams. To a lesser extent, some of the water is also used for irrigation or drinking water. Similar results were also found in previous studies in the Rhone and Garonne basins [*Etchevers et al.*, 2001a, 2001b, 2002; *Habets et al.*, 1999c; *Voirin-Morel*, 2003]. In the upper mountains, there is relatively little water extraction, and most of the water is simply stored in reservoirs for hydropower. This is not the case in the lower Durance, where a significant part of the water is diverted for irrigation and drinking water. It can be seen in Figure 11 for the Alps that although the efficiency is poor, the discharge is well estimated with an error below 10%. Poor results in the two rivers in the northern part of France are due to the fact that a large aquifer which is closely connected to the rivers is not yet simulated by SIM. The discharge is underestimated in one of the two rivers, and it is estimated quite well for the other one. Except for these two regions, the results are quite homogeneous over all of France.

[50] As the simulated period covers contrasting climates, it is of interest to look at the time evolution of the statistical results. In order to be able to compare the statistics from year to year, it is essential to have a homogeneous set of river gauge time series. Therefore, the river gauges with more than 200 d of observations available each year were selected. Moreover, in order to be able to aggregate the results, another criterion was added: the efficiency should be positive each year. There are 140 river gauges that fit these criteria. The corresponding results are presented in Figure 12 for five large basins, and on average for all of France. The discharge ratio and the efficiency are shown, together with their regression fits which give the overall tendency. The statistical results vary from year to year. In addition, they also vary from one basin to the next, but there are some common characteristics when looking at the efficiency: the best results are obtained in the year 2002–2003, while the worst are found in one of the 3 following years: 1995–1996, 2001–2002, or 2004–2005. The results are less homogeneous in terms of the discharge ratio. It tends to decrease during the entire time period for the Loire and Garonne basins, leading to a reduction of the error on the Loire, and to an increase on the Garonne. There is no clear signal in the Rhone and Seine basins. Over all of the France, there is a slight tendency for the discharge ratio decrease, with an underestimation around 8% at the end of the period. In general, there is no clear relation between the efficiency and the error in the discharge of a given year. However, it appears that the model obtains worst results in terms of efficiency during the driest years. This is clearly seen in Figure 13 where the observed annual discharge is shown along with the resulting efficiency on the average for

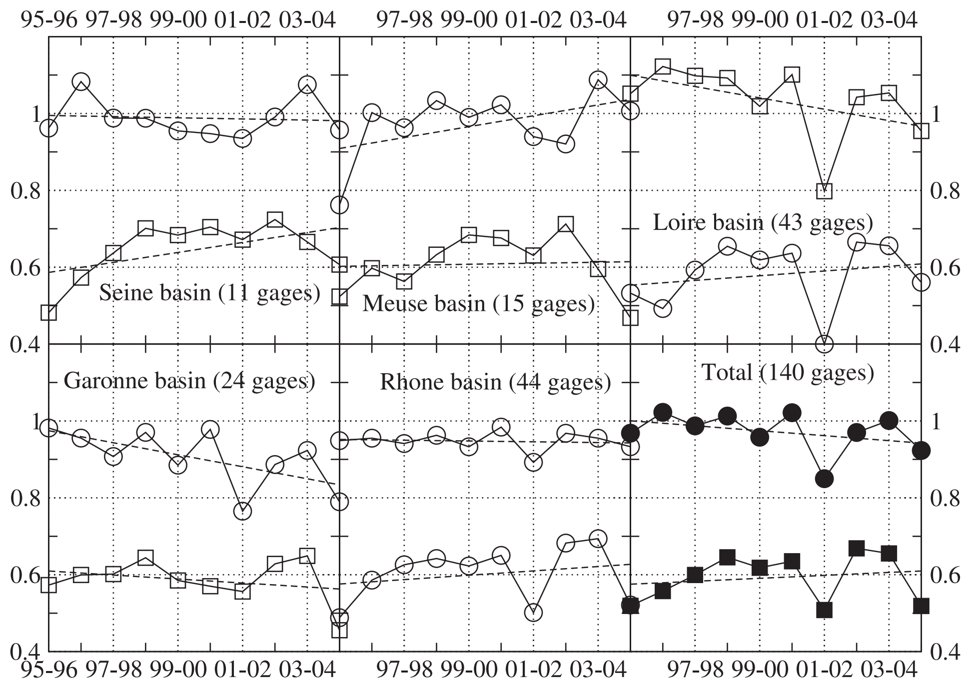

Figure 12. Evolution of the efficiency (circles) and discharge ratio (squares) on average on five large basins and on average for all of France. Only the river gauges with more than 200 d available each year (and with positive values of the efficiency) were taken into account. Their number is indicated on the plots.

each of the five basins and for all the selected stations. The difficulty with dry periods can have several explanations: (1) the low flows are sustained by the various water tables, and only a few of them are explicitly represented in SIM, (2) processes associated with dryness or low soil moisture are perhaps poorly simulated by the SIM model, and (3) part of the error is probably due to the human management of the river (not taken into account by SIM), since both the effect of the dams, and the pumping in rivers or from the water tables have more impact during the period of low flow. However, Figure 13 shows that although the results tend to improve when the observed discharge increases, the best results are not obtained for the wettest year.

4.2. Comparison With Observed Piezometric Head

[51] Piezometric head is thoroughly monitored in France, and numerous data are available. For the Seine basin, the

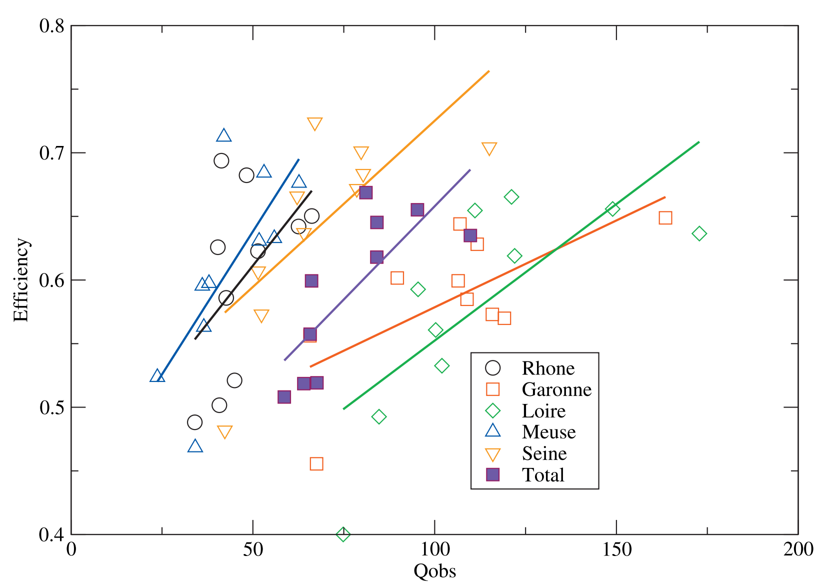

Figure 13. Relation between the efficiency and the observed discharge on average on the selected river gauges of each basin. The lines correspond to the linear regression for a given basin.

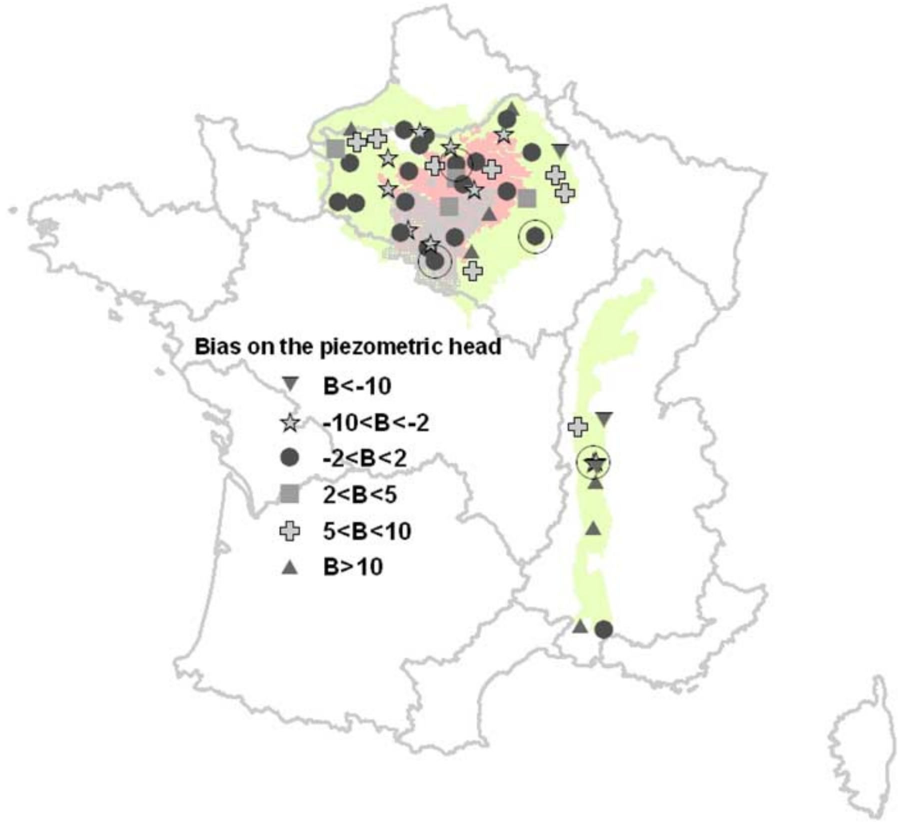

Figure 14. Spatial distribution of the bias on the 10-year simulation of the piezometric head simulated by SIM.

piezometric gages were selected in order to keep only the representative ones, i.e., those that are not impacted by pumping, and those that are not too close to a river. Thus, 43 observation sites were chosen, with data available for the 10-year study period. Such a selection was more difficult in the Rhone basin because the water table is along the river: therefore only eight gages were retained. The location of the selected piezometric gages as well as the average bias between the simulation and the observation of the piezometric head are shown in Figure 14. There are some points where the absolute bias is above 10 m, especially for the Rhone basin. However, there are 20 gages for which the absolute bias is lower than 2 m. One such gage is located in the Rhone basin, and the other ones are spread over the three aquifer layers of the Seine basin. Figure 15 presents the comparison between observed and the simulated piezometric head for the four gages encircled in Figure 14. The amplitude of variation of the Rhone aquifer at Genas is rather weak, because the aquifer level is constrained by the river. For the Seine basin, the annual amplitude varies from gage to gage. However, for almost every gage, there is an increase of the piezometric head during the wet year 2000–2001, and a clear decrease in 2003–2004. These evolutions are well captured by the model.

4.3. Comparison With the Observed Snow Depth

[52] The snow accumulation and melt are key components of the water and energy budgets. The comparison with observed and simulated snow depths is possible at some meteorologic observing stations and at numerous mountain sites. In order to be sure of the quality of the observed data set, only the stations that observed at least 30 d of nonzero snow depth during the 10-year period are selected. Moreover, the comparison between observations and the simulation are made only if the altitude of the grid cell is close to that of the station (less than 150 m difference). With this selection criteria, 505 stations with snow depth measurements were selected. As the snow cover depends mostly on the altitude in France, Figure 16 presents the daily

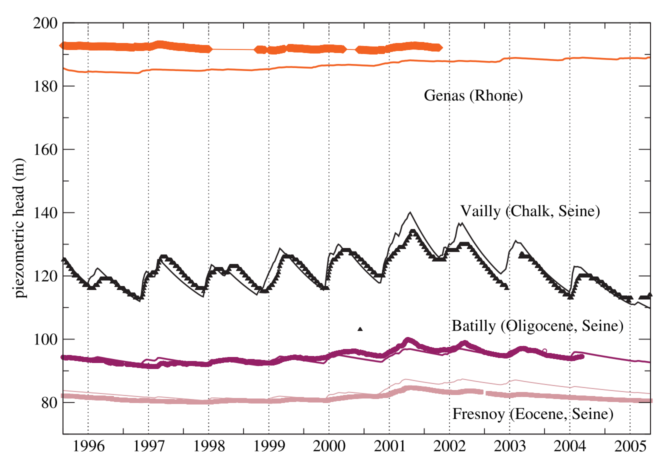

Figure 15. Evolution of the observed (symbol) and simulated (line) piezometric head for one given station over each layer of the Seine and Rhone aquifers.

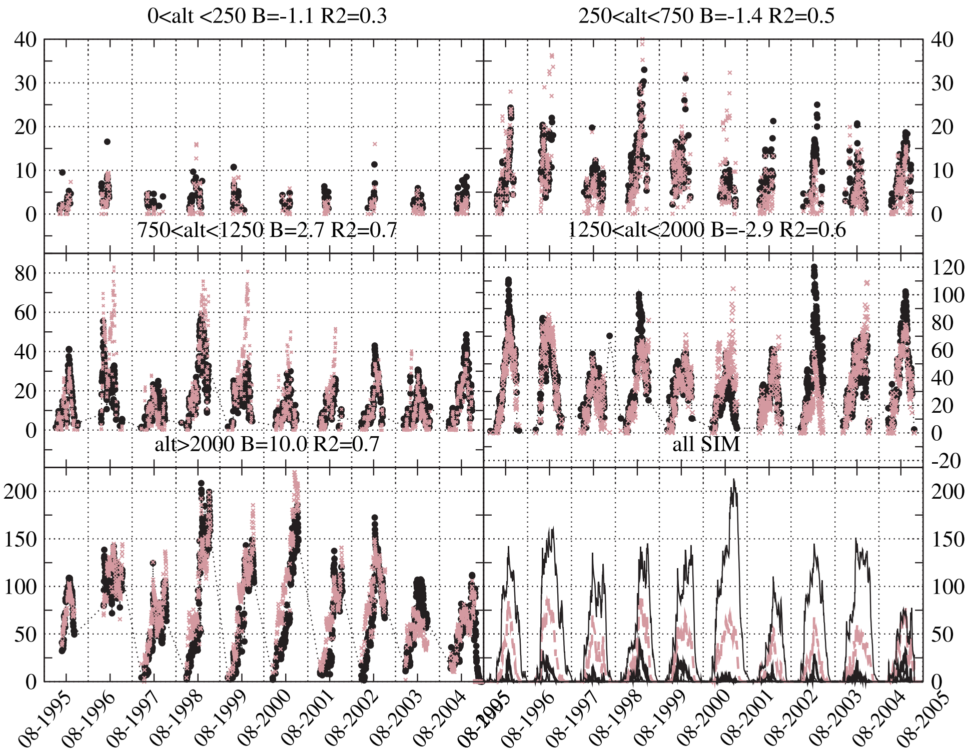

Figure 16. Snow depth observed (black dots) and simulated (crosses) average on several gages according to their altitude (the average is computed each day on the stations with available data). The bottom right panel presents the evolution of the simulated snow depth on the selected stations of the four levels (the same number of stations is used each day to compute the average). Levels 750–1250 m black thick line; 1250–2000 gray line; over 2000 m thin black line. The square correlation (R2) and the bias in cm (B) are given in the footers.

comparison between observed and simulated snow depths for altitude bands. The number of station varies for each level from 19 for the upper level (above 2000 m) to 179 for the level 250–750 m. However, the observations are not available each day at all stations, so that the number of stations used to compute the average varies from day to day (with a minimum of two stations). As expected, the snowpack generally lasts longer and is deeper as the altitude increases. The snowpack has large interannual variations which vary at each level. However, the plotted evolution is affected by the number of gages used to compute the average which vary each day. In order to be able to estimate the temporal evolution of the snowpack, the snow depth simulated by SIM on average for all the stations selected for each level is presented in the bottom left panel of Figure 16. In Figure 16, the same number of points are used everyday, thus leading to a real temporal evolution. The bias and the squared correlation between observation and simulation are given in Figure 16. The model is able to reproduce the observed evolution of the snowpack. The bias is rather low on average (around 3 cm up to 10 cm at the highest level), even if the error can be large at times. The squared correlation is low for the lowest level where the snowpack does not last long, and reaches 0.7 at the highest level. Figure 17 presents about the same data set but on an annual basis. The annual evolution of the snowpack is well estimated by the model, with the squared correlation which reaches 0.9 for all levels except the lowest one. However, there are systematic errors in the two highest levels: an underestimation of the snow depth from January to February for the level 1250–2000 m, and, in contrast an overestimation of the snow depth from September to January for the level above 2000 m, and during the melting period in May–June. It is difficult to estimate how such systematic error may affect the water budget and the simulation of the streamflows, since those results are affected by the availability of the observations. For instance, it can be seen on the lower right panel that the maximum snow depth is simulated in February, whereas it appears to be in early May in the comparison with the observations for the upper level.

4.4. Water and Energy Budgets at the Basin Scale

[53] The simulated annual water and energy budgets can be partially assessed using the comparison between observed and simulated discharges. For that, there is a focus only on the largest subbasins, using the river gauges with the longest observation periods. Figure 18 presents the results for the four main basins (Rhone at Beaucaire, Seine at Paris, Garonne at Tonneins, and Loire at Nantes). For these basins, the discharge error for the whole period represents +63, +24, −15, and +50 m^3/s, which corresponds to an average error in mm/a of +26, +18, −10, +14, respectively (see Table 1). The error for the Rhone basin is the largest. This is due in part to the large anthropogenic impact, which consists in numerous dams and canals in the Durance and Isere river basins. For instance, in 2003 in the

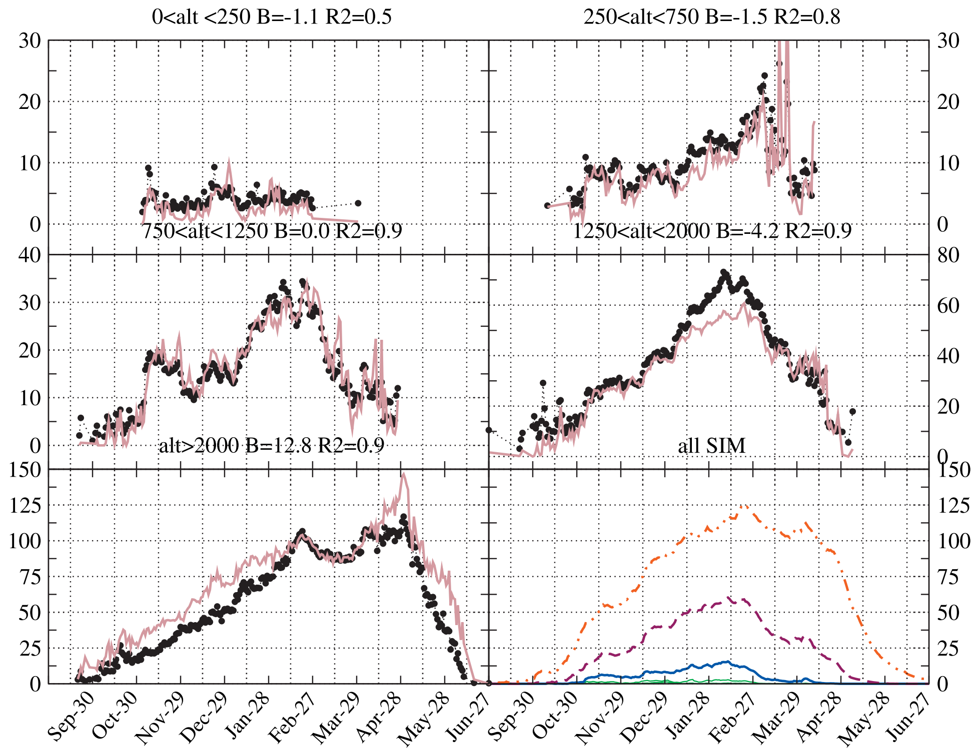

Figure 17. Same as Figure 16 but on average on an annual cycle.

Durance subbasin, the total quantity of water derived to sustain human activities (irrigation, drinking water, cooling of energy plants, etc.) was 37 m^3/s, which represents approximately half of the error at Beaucaire for this single subbasin (data available at http://sierm.eaurmc.fr/telechargement/bibliotheque.php?categorie=prelevements). However, it is difficult to estimate which part of this water is going back to the river network.

[54] A simple estimation of the evaporation error at the basin scale can be made by assuming that all of the discharge error only results from evaporation. This implies several strong hypotheses: (1) there is no error in the precipitation at the basin scale, (2) there is no error in the observations of the river flow, (3) there is no error in terms of the estimation of the water storage in the soil, the snowpack, the aquifers and the rivers at the annual scale, and (4) the water storage in the dams is not significant on a annual scale. Using this estimated error, it is possible to analyze the spatial and temporal evolution of the water and energy budgets.

[55] The annual evaporation is quite similar for the four basins, ranging from 573 mm/a on average for the Seine basin to 634 mm/a on average for the Garonne, with an annual amplitude of about ±100 mm/a (which is quite smooth over the 10-year period, Table 1). On average over the 10-year period, the estimated evaporation error represents about 4% of the annual flux. However it varies from year to year, and can reach 8% of the annual evaporation and even 15% in the Rhone basin in 2000–2001 (Table 1). The Rhone basin is the only large basin for which the total runoff is about the same magnitude as the evaporation (about 590 mm/a). For the other basins, the total runoff is about 2 times lower than the evaporation. The evolution of the annual runoff is less smooth than the annual evaporation and more closely follows the annual variation of the precipitation.

[56] In terms of the energy budget, only the latent heat flux error can be estimated, and one cannot determine how this error affects the sensible, ground heat and the net radiation fluxes. Thus, the estimated latent heat flux error is presented independently of the other energy budget terms. This error, expressed in W/m^2, varies from -0.8 W/m^2 in the Garonne basin to 1.7 W/m^2 in the Rhone basin. It is striking that the error estimated on the latent heat flux roughly accounts for 10% of the sensible heat flux, and that they are of the same order of magnitude in the Rhone basin in 2000–2001. Indeed, the averaged annual sensible heat flux ranges between 15.3 W/m^2 in the Rhone basin to 19 W/m^2 in the Loire basin. Its annual evolution can be rather smooth as in the Rhone basin (from 10 to 20 W/m^2) or more pronounced as in the Seine basin (from 6 to 30 W/m^2). The net radiation is 10% larger in the Garonne basin than in the Seine or Rhone basins. But for all of the basins, the annual evolution of the net radiation is quite smooth, with a total amplitude of ±6%.

[57] Figure 19 shows maps of the Bowen ratio and the ratio of the evaporation to precipitation. The two maps show large contrasts over France. The largest value of the Bowen ratio are along the southern Alps (where the snowfall is significant, thus limiting the evaporation, but where the incoming radiation fluxes are large), along the Mediterranean coast (including Corsica), and for two areas along the west coast. Half of the areas where the Bowen ratio is above 0.75 correspond to areas where the average annual rainfall is below 650 mm/a or where the net radiation is above 80 W/m^2. The residual is mostly located in Corsica and along the

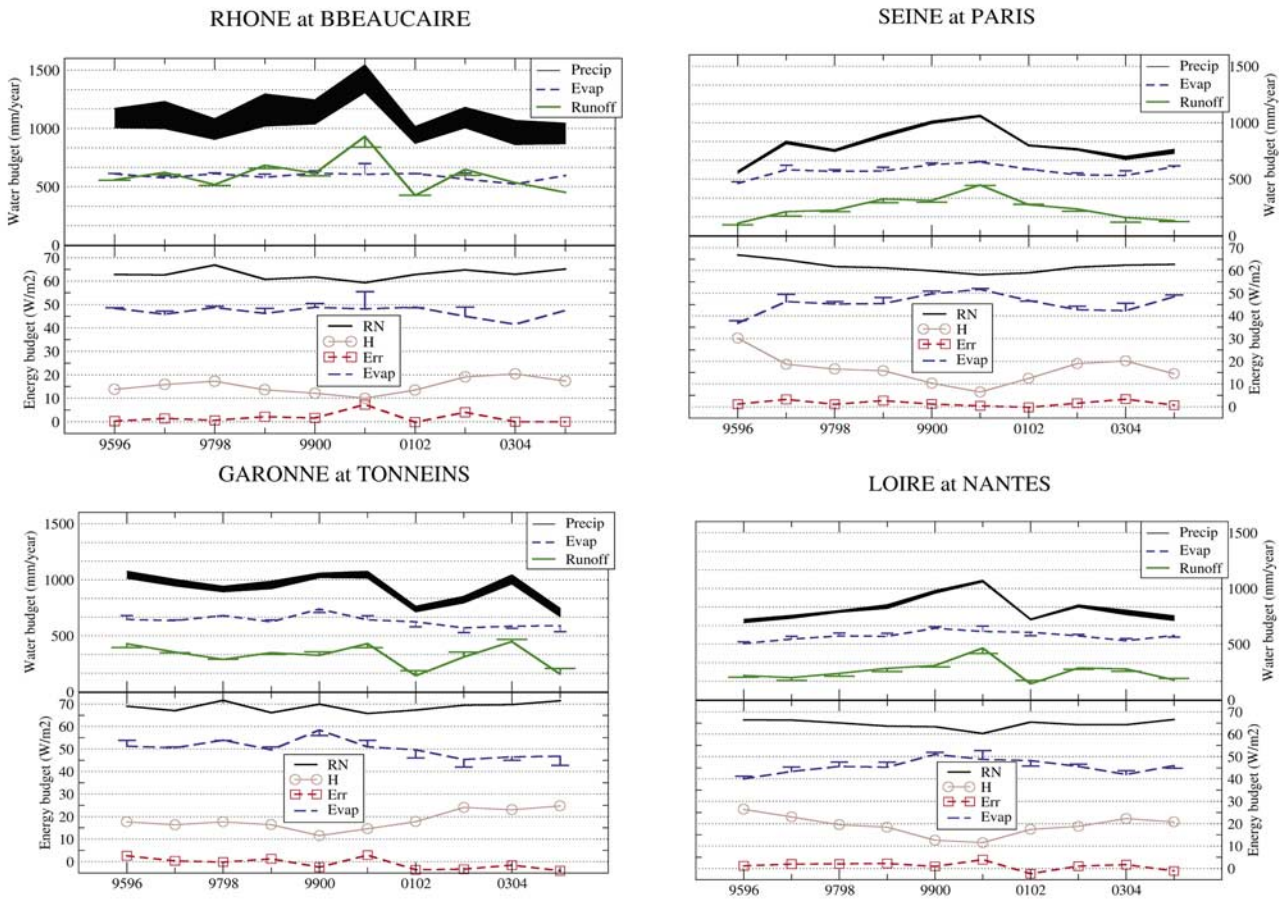

Figure 18. Water and energy budgets over the four main basins. The thick black line is the total precipitation (Precip), and its thickness represents the snowfall. Evaporation (Evap), total runoff (Runoff) and latent heat flux (LEW) have an error bar that was estimated according to the error between the observed and simulated discharge. This error is shown in the energy budget panel (bottom) (Err) in order to compare with the net radiation (RN) and the sensible heat flux (H).

eastern Mediterranean coast, and corresponds to the regions where the precipitation can be intense. Here, relatively few rain events produce large amounts of precipitation primarily during the fall season, and they produce large proportion of runoff, thereby reducing the evaporation rate. This is also the reason why the evaporation in this Mediterranean region represents less than 75% of the precipitation, even in areas where the precipitation is lower than 650 mm/a, as is the

Table 1. Main Characteristics of the Water Budget of the Four Main Basins[a]

	Basin			
	Rhone Beaucaire	Seine Paris	Garonne Tonneins	Loire Nantes
Surface (km^2)	96,412	43,509	50,430	112,187
P (mm/a)	1189	820	956	834
E (mm/a)	590	573	634	574
RO (mm/a)	599	243	324	259
Err (mm/a)	26	18	−10	14
Err/E (%)	4.4	3.1	1.6	2.4
Max annual Err (mm/a)	92	42	−51	49
Max annual Err/E (%)	15	8	−9	8
Year max annual error	2000–2001	2003–2004	2004–2005	2000–2001
Err (W/m^2)	1.7	1.5	−0.8	1.1
RN (W/m^2)	63.0	61.8	68.7	64.5
H (W/m^2)	15.3	16.4	18.4	19.1
LE (W/m^2)	46.9	45.6	50.3	45.6

[a]E, mean annual evaporation; RO, mean annual total runoff; Err, averaged 10-year annual error computed with the observed river flow (in mm/a and in W/m^2); Err/E, percentage of the error compared to the mean annual evaporation; max Err, maximal annual error on the 10-year period, estimated with the observed river flow; max Err/E, percentage of this maximal error compared to the annual evaporation of the year; year max, year where the error is maximal; RN, net radiation; H, sensible heat flux; LE, latent heat flux.

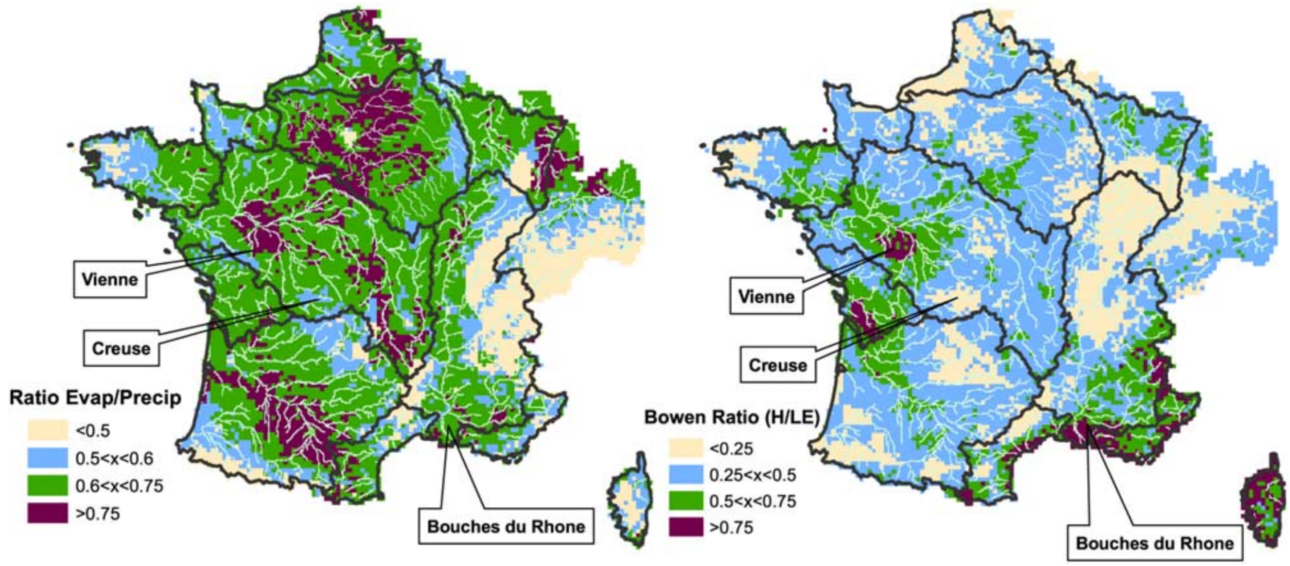

Figure 19. (left) The 10-year average bowen ratio (H/LE) and (right) 10-year average ratio of the evaporation to precipitation.

case for instance in the "Bouches du Rhone" site indicated in Figure 19. In contrast, the area in the Vienne department (see flag on the maps) has both a large value of the Bowen ratio and of the ratio of the evaporation to precipitation. The other areas, where at least 75% of the precipitation evaporates, are located around the Seine basin and the Garonne Valley. Such results are consistent with those obtained by *Rousset et al.* [2004] and *Voirin-Morel* [2003], respectively, for different time periods than examined in the current study.

[58] Figure 20 shows the time evolution of the soil wetness index for the three points indicated in Figure 19. In addition to the sites in the Vienne and Bouches du Rhone departments, one site in the Creuse department was selected as being representative of a weak Bowen ratio and an average E/P ratio. The 10-year average value of the fluxes for these three sites are given in Table 2. The soil wetness index is computed from the expression soil wetness index (SWI) = $(w_{tot} - w_{wilt})/(w_{fc} - w_{wilt})$, where w_{tot} is the volumetric water content of the simulated soil column, w_{fc} is the field capacity, and w_{wilt} the wilting point. Thus, a value of the soil wetness index above 1 indicates that there is no evaporative water stress, and a value of 0 indicates that plant transpiration has ceased. At Creuse site the minimum value of the SWI in summer is the highest (just below 0.25 in 2003 and close to 0.5 in 1997), which indicates a moderate water stress for the vegetation. On the other hand, the water stress is significant in summer at the Bouches du Rhone site, with a SWI below 0.1 during 4 years out of 10, and a minimal value below 0.02 reached during the exceptionally hot and dry summer of 2003. At the Vienne site, the summer value of the SWI is around 0.17, with a minimum value of 0.12 in 2005 after a dry winter. In winter time, the maximum value of the SWI is below 1, meaning that there is a water stress in winter 5 years out of 10 in the Bouches du Rhone site, and 2 years out of 10 in the Vienne site. Such a pattern does not occur at the Creuse site.

[59] The encapsulated graph in Figure 20 represents the mean annual evolution of the soil moisture. The Creuse and Vienne sites have similar temporal evolutions, with a drier

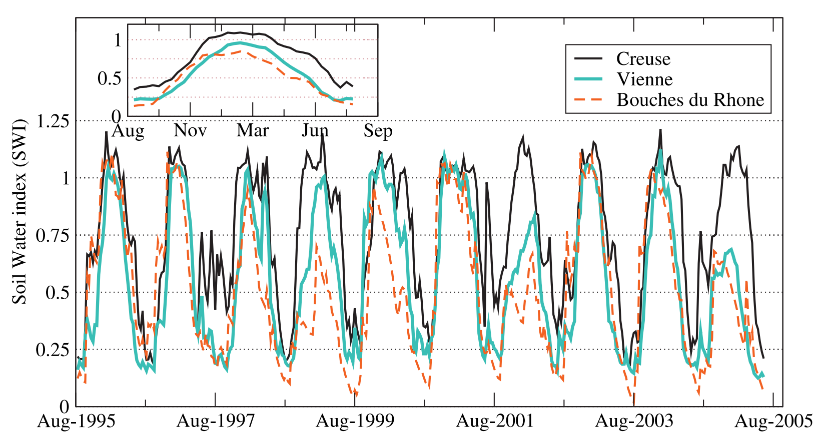

Figure 20. The 10-d evolution of the soil water index (SWI) on the three sites plotted in Figure 19. The inset graph is the annual average.

Table 2. Mean Annual Water and Energy Budget on the Three Grid Cells Indicated in Figure 19[a]

Site	Precip (mm/a)	Evap (mm/a)	H (W/m^2)	LE (W/m^2)	RN (W/m^2)	E/P	H/LE
Vienne	637	507	34	40	76	0.80	0.88
Bouches du Rhone	650	428	29	34	63	0.65	0.86
Creuse	1167	675	12	53	65	0.58	0.22

[a]Precip, total precipitation; Evap, evapotranspiration; H, sensible heat flux; LE, latent heat flux (same as Evap, but expressed in W/m^2); RN, net radiation; E/P, ratio of the evaporation over the precipitation; H/LE, Bowen ratio.

soil at Vienne (0.55 on average) compare to Creuse (0.75 on average). The temporal evolution of the SWI is slightly shifted in the Bouches du Rhone site, with an increase of the SWI starting early September due to significant precipitation, and the maximum value is reached in November, with a 10-year average value of 0.5.

[60] Another interesting result which can be obtained with the SIM system is the evaluation of the total volume of the water that reaches the Mediterranean sea, via the large rivers but also the smallest. This is of interest since this component of the water budget of the Mediterranean sea is not well known. The simulated hydrographic network takes into account 80 rivers that flow to the Mediterranean Sea (30 are located in Corsica), and only 30 of them have a basin larger than 250 km^2. According to the simulation, 2287 m^3/s flows to the Mediterranean sea on average every year. 80% of this flow is from the Rhone river, and 91% by the 10 largest Mediterranean rivers (two being located in Corsica). Most of those Mediterranean rivers are located in mountainous regions, characterized by a significant snow cover in winter, leading to a smaller fraction of the precipitation that evaporates (55% on average).

5. Conclusion

[61] The hydrometeorological model SAFRAN-ISBA-MODCOU (SIM) was extended to all of France in order to have a homogeneous estimation nationwide of the water resource. The 10-year simulation was compared with daily river flow, piezometric head, and snow depth observations. SIM obtained reasonable results (efficiency above 0.55) for more than 66% of the 610 river gauges simulated, and rather good results (efficiency above 0.65) for more than 36% of them. It was found that worse results were obtained during the driest years, which is more likely due to the fact that only few aquifers are simulated explicitly.

[62] These comparisons show that SIM is quite robust both in space and time and gives a good estimation of the water fluxes. As the ISBA surface scheme is used in weather forecast and climate models, it is important to estimate the quality of the simulated latent heat flux. The comparison with the observed river flow, associated with some hypotheses, permits an estimation that the error is less than 4% on annual average.

[63] Since 2003, the SIM system has been used operationally at Météo-France: for each D, it performs an atmospheric analysis and hydrological simulation of day D-1. It is the first time that such a system is used to monitor the water budget of France in real time, and especially, to estimate the soil wetness. The soil wetness can be used to estimate the flood risk, or to monitor the spatial and temporal evolution of a drought. Such information is now part of the national hydrological bulletin of the French environment ministry (http://www.eaufrance.fr), which is published monthly.

[64] The SIM operational application is also used to prescribe the initial condition for an ensemble river flow forecasts system over all of France. The 10-d ensemble precipitation forecast are taken from the European Centre for Medium-Range Weather Forecasts (ECMWF), and then disaggregated in space. They are then employed as an input for the ISBA-MODCOU hydrometeorological system to make 10-d forecasts of the river flows [*Rousset-Regimbeau et al.*, 2006, 2007, available at http://www.ecmwf.int/publications/newsletters/pdf/111.pdf].

[65] As in the NLDAS and CALDAS projects [*Mitchell et al.*, 2004; *Balsamo et al.*, 2006], the operational hydrometeorological model SIM can also be used to prescribe the initial soil moisture conditions of a mesoscale weather model. Some first attempts have been made with the Meso-NH mesoscale model [*Donier et al.*, 2003] and such an approach could be generalized in the near future.

[66] It is planned to increase the period of time covered by the SIM system in order to be able to use it for climatological and statistical analyses. For instance, in the Seine basin, 18 years of the SAFRAN analysis were used with the ISBA-MODCOU hydrometeorological model in studies by *Boé et al.* [2006, 2007] in order to disaggregate in space and time the simulation of a climate model. It was also used estimate the ability of this climate model to reproduce the observed present day conditions.

[67] **Acknowledgments.** We would like to thank the French National Program for the Research in Hydrology (PNRH) for its financial support in this action.

References

Artinyan, E., F. Habets, J. Noilhan, E. Ledoux, D. Dimitrov, E. Martin, and P. Le Moigne (2008), Modelling the water budget and the riverflows of the Maritsa basin in Bulgaria, *Hydrol. Earth Syst. Sci.*, *12*, 21–37.

Balsamo, G., J. F. Mahfouf, S. Bélair, and G. Deblonde (2006), A global root-zone soil moisture analysis using simulated L-band brightness temperature in preparation for the Hydros satellite mission, *J. Hydrometeorol.*, *7*, 1126–1146.

Benoit, R., P. Pellerin, N. Kouwen, H. Ritchie, N. Donaldson, P. Joe, and E. D. Soulis (2000), Toward the use of coupled atmopspheric and hydrologic models at regional scale, *Mon. Weather Rev.*, *128*, 1681–1706.

Boé, J., L. Terray, F. Habets, and E. Martin (2006), A simple statistical-dynamical downscaling scheme based on weather types and conditional resampling, *J. Geophys. Res.*, *111*, D23106, doi:10.1029/2005JD006889.

Boé, J., L. Terray, F. Habets, and E. Martin (2007), Statistical and dynamical downscaling of the Seine basin climate for hydrometeorological studies, *Int. J. Climatol.*, *27*(12), 1643–1655.

Boone, A., and P. Etchevers (2001), An inter-comparison of three snow schemes of varying complexity coupled to the same land-surface model: Local scale evaluation at an Alpine site, *J. Hydrometeorol.*, *2*, 374–394.

Boone, A., J. C. Calvet, and J. Noilhan (1999), Inclusion of a third soil layer in a land surface scheme using the force-restore method, *J. Appl. Meteorol.*, *38*, 1611–1630.

Boone, A., et al. (2004), The Rhone-aggregation land surface scheme intercomparison project: An overview, *J. Clim.*, *17*(1), 187–208.

Caballero, Y., S. Voirin-Morel, F. Habets, J. Noilhan, P. Le Moigne, A. Lehenaff, and A. Boone (2007), Hydrological sensitivity of the Adour-Garonne river basin to climate change, *Water Resour. Res.*, *43*, W07448, doi:10.1029/2005WR004192.

Chen, F., Z. Janjic, and K. Mitchell (1997), Impact of atmopsheric surface layer parameterizations in the new land-surface scheme of the NCEP mesoscale Eta model, *Bounday Layer Meterol.*, *85*, 391–421.

Donier, S., F. Habets, P. Lacarrère, P. Le Moigne, and J. Noilhan (2003), Initialisation of soil moisture in mesoscale atmospherical model, *Geophys. Res. Abstr.*, *5*, 05467.

Durand, Y., E. Brun, L. Merindol, G. Guyomarc'h, B. Lesaffre, and E. Martin (1993), A meteorological estimation of relevant parameters for snow models, *Ann. Geophys.*, *18*, 65–71.

Etchevers, P., Y. Durand, F. Habets, E. Martin, and J. Noilhan (2001a), Impact of spatial resolution on the hydrological simulation of the Durance high-Alpine catchment, France, *Ann. Glaciol.*, *32*, 87–92.

Etchevers, P., C. Golaz, and F. Habets (2001b), Simulation of the water budget and the river flows of the Rhone basin from 1981 to 1994, *J. Hydrol.*, *244*, 60–85.

Etchevers, P., C. Golaz, F. Habets, and J. Noilhan (2002), Impact of a climate change on the Rhone river catchment hydrology, *J. Geophys. Res.*, *107*(D16), 4293, doi:10.1029/2001JD000490.

Golaz-Cavazzi, C., P. Etchevers, F. Habets, E. Ledoux, and J. Noilhan (2001), Comparison of two hydrological simulations of the Rhone basin, *Phys. Chem. Earth, Part B*, *26*(5–6), 461–466.

Gomez, E., E. Ledoux, P. Viennot, C. Mignolet, M. Benoit, C. Bornerand, C. Schott, B. Mary, G. Billen, A. Ducharne, and D. Brunstein (2003), An integrated modelling tool for nitrates transport in a hydrological system: Application to the river Seine Basin, *Houille Blanche*, *3*, 38–45.

Habets, F., P. Etchevers, C. Golaz, E. Leblois, E. Ledoux, E. Martin, J. Noilhan, and C. Ottle (1999a), Simulation of the water budget and the river flows of the Rhone basin, *J. Geophys. Res.*, *104*, 31,145–31,172.

Habets, F., J. Noilhan, C. Golaz, J. P. Goutorbe, P. Lacarrere, E. Leblois, E. Ledoux, E. Martin, C. Ottle, and D. Vidal-Madjar (1999b), The Isba surface scheme in a macroscale hydrological model applied to the Hapex-Mobilhy area. part I: Model and database, *J. Hydrol.*, *217*, 75–96.

Habets, F., J. Noilhan, C. Golaz, J. P. Goutorbe, P. Lacarrere, E. Leblois, E. Ledoux, E. Martin, C. Ottle, and D. Vidal-Madjar (1999c), The Isba surface scheme in a macroscale hydrological model applied to the Hapex-Mobilhy area. part I: Simulation of streamflows and annual water budget, *J. Hydrol.*, *217*, 97–118.

Henriksen, H., L. Troldborg, P. Nyegaard, T. Sonnenborg, J. Refsgaard, and B. Madsen (2003), Methodology for construction, calibration and validation of a national hydrological model for Denmark, *J. Hydrol.*, *280*, 52–71.

Ivanov, V. Y., E. R. Vivoni, R. L. Bras, and D. Entekhabi (2004), Catchment hydrologic response with a fully distributed triangulated irregular network model, *Water Resour. Res.*, *40*, W11102, doi:10.1029/2004WR003218.

Ledoux, E., G. Girard, G. De Marsily, and J. Deschenes (1989), Spatially distributed modeling: Conceptual approach, coupling surface water and ground-water, in *Unsaturated Flow Hydrologic Modeling: Theory and Practice*, *NATO ASI Series C*, vol. 275, edited by H. J. Morel-Seytoux, pp. 435–454, Kluwer Acad., Norwell, Mass..

Liang, X., D. P. Lettenmaier, E. F. Wood, and S. J. Burges (1994), A simple hydrologically based model of land surface water and energy fluxes for general circulation models, *J. Geophys. Res.*, *99*(D7), 14,415–14,428.

Lohmann, D., et al. (1998), The Project for Intercomparison of Land-surface Parameterization Schemes (PILPS) phase 2(c) Red-Arkansas River basin experiment: 3. Spatial and temporal analysis of water fluxes, *Global Planet. Change*, *19*(1–4), 161–179.

Masson, V., J. L. Champeaux, F. Chauvin, C. Meriguet, and R. Lacaze (2003), A global database of land surface parameters at 1 km resolution in meteorological and climate models, *J. Clim.*, *16*, 1261–1282.

Miller, J. R., L. G. Russel, and G. Caliri (1994), Continental scale river flow in climate models, *J. Clim.*, *7*, 914–928.

Mitchell, K. E., et al. (2004), The multi-institution North American Land Data Assimilation System (NLDAS): Utilizing multiple GCIP products and partners in a continental distributed hydrological modeling system, *J. Geophys. Res.*, *109*, D07S90, doi:10.1029/2003JD003823.

Nash, J. E., and J. V. Sutcliffe (1970), River flow forecasting through conceptual models, *J. Hydrol.*, *10*(3), 282–290.

Noilhan, J., and P. Lacarrère (1995), GCM gridscale evaporation from mesoscale modeling, *J. Clim.*, *8*(2), 206–223.

Noilhan, J., and J.-F. Mahfouf (1996), The ISBA land surface parameterization scheme, *Global Planet. Change*, *13*, 145–159.

Noilhan, J., and S. Planton (1989), A simple parameterization of land surface processes for meteorological models, *Mon. Weather Rev.*, *117*, 536–549.

Quintana Seguí, P., P. Le Moigne, Y. Durand, E. Martin, F. Habets, M. Baillon, L. Franchisteguy, S. Morel, and J. Noilhan (2008), Analysis of near-surface atmospheric variables: Validation of the SAFRAN analysis over France, *J. Appl. Meteorol. Climatol.*, *47*(1), 92–107.

Reed, S., V. Koren, M. Smith, Z. Zhang, F. Moreda, and D.-J. Seo (2004), Overall distributed model intercomparison project results, *J. Hydrol.*, *298*, 27–60.

Ritter, B., and J. F. Geleyn (1992), A comprehensive radiation scheme for numerical weather prediction models with potential applications in climate simulations, *Mon. Weather Rev.*, *120*, 303–325.

Rousset, F., F. Habets, E. Gomez, P. Le Moigne, S. Morel, J. Noilhan, and E. Ledoux (2004), Hydrometeorological modeling of the Seine basin using the SAFRAN-ISBA-MODCOU system, *J. Geophys. Res.*, *109*, D14105, doi:10.1029/2003JD004403.

Rousset-Regimbeau, F., F. Habets, and E. Martin (2006), Ensemble streamflow forecast over the entire France, *Geophys. Res. Abstr.*, *8*, 01962.

Rousset-Regimbeau, F., F. Habets, E. Martin, and J. Noilhan (2007), Ensemble streamflow forecasts over France, *ECMWF Newsl.*, *111*, 21–27.

Voirin-Morel, S. (2003), Modélisation distribuée des flux d'eau et d'énergie et des débits à l'échelle régionale du bassin Adour Garonne, Ph.D. thesis, 292 pp., Univ. Paul Sabatier-Toulouse III, Toulouse, France.

Willmot, C. J. (1981), On the validation of models, *Phys. Geog.*, *2*, 184–194.

Wood, E. F., et al. (1998), The Project for Intercomparison of Land-Surface Parameterization Scheme (PILPS) Phase-2(c) Red-Arkansas river experiment: I. Experiment description and summary intercomparisons, *Global Planet. Change*, *19*, 115–135.

A. Boone, J. L. Champeaux, L. Franchistéguy, P. Le Moigne, E. Martin, J. Noilhan, P. Quintana Seguí, and F. Rousset-Regimbeau, GAME/CNRM, Météo-France, CNRS, 42 avenue Coriolis, F-31057 Toulouse, France.

P. Etchevers, CEN, Météo-France 1441, rue de la Piscine Domaine Universitaire, F-38406 Saint-Martin-d'Heres Cedex, France.

F. Habets, UMR-Sisyphe 7619, Universit Pierre-et-Marie Curie Paris VI, Boite 123, 4 place Jussieu, F-75252 Paris Cedex 05, France. (florence.habets@ensmp.fr)

E. Leblois, CEMAGREF 3 B, Quai Chauveau, F-69009 Lyon, France.

E. Ledoux and P. Viennot, Centre de Geosciences, ENSMP, ParisTech, 35 rue St honoré, F-77305 Fontainebleau, France.

S. Morel, DIRIC, Météo-France, 2, avenue Rapp, F-75007 Paris, France.